Candidatus Nitrosopolaris, a genus of putative ammonia-oxidizing archaea with a polar/alpine distribution

Igor S. Pessi[1,2], Aino Rutanen[1], and Jenni Hultman[1,2,3*]

[1]Department of Microbiology, University of Helsinki, Helsinki, Finland
[2]Helsinki Institute of Sustainability Science (HELSUS), Helsinki, Finland
[3]Natural Resources Institute Finland (LUKE), Helsinki, Finland
[*]Corresponding author: jenni.hultman@helsinki.fi

Abstract

Ammonia-oxidizing archaea (AOA) are key players in the nitrogen cycle of polar soils. Here, we analysed metagenomic data from tundra soils in Rásttigáisá, Norway, and recovered four metagenome-assembled genomes (MAGs) assigned to the genus "UBA10452", an uncultured lineage of putative AOA in the order Nitrososphaerales ("terrestrial group I.1b"), phylum Thaumarchaeota. Analysis of other eight previously reported MAGs and publicly available amplicon sequencing data revealed that the UBA10452 lineage is predominantly found in acidic polar and alpine soils. In particular, UBA10452 MAGs were more abundant in highly oligotrophic environments such as mineral permafrost than in more nutrient-rich, vegetated tundra soils. UBA10452 MAGs harbour multiple copies of genes related to cold tolerance, particularly genes involved in DNA replication and repair. Based on the phylogenetic, biogeographical, and ecological characteristics of 12 UBA10452 MAGs, which include a high-quality MAG (90.8% complete, 3.9% redundant) with a nearly complete 16S rRNA gene, we propose a novel *Candidatus* genus, *Ca.* Nitrosopolaris, with four species representing clear biogeographical/habitat clusters.

Introduction

Nitrification – the oxidation of ammonia to nitrite and further oxidation to nitrate – is a crucial part of the nitrogen (N) cycle providing a link between reduced and oxidized forms of N. The first step of nitrification, ammonia oxidation, is carried out mainly by aerobic chemolithoautotrophic microorganisms that grow by coupling the energy obtained from the oxidation of ammonia with carbon dioxide (CO_2) fixation (Lehtovirta-Morley, 2018). Ammonia-oxidizing archaea (AOA) outnumber ammonia-oxidizing bacteria (AOB) by orders of magnitude

in many terrestrial and aquatic environments, particularly in oligotrophic environments with low N input (Leininger *et al.*, 2006; Schleper and Nicol, 2010; Lehtovirta-Morley, 2018). Among the reasons for their ecological success is an enzymatic machinery with higher affinity for ammonia and a more efficient CO_2 fixation pathway than their bacterial counterparts (Martens-Habbena *et al.*, 2009; Könneke *et al.*, 2014; Kerou *et al.*, 2016). However, high ammonia affinity is not a common trait to all AOA, with some strains displaying a low substrate affinity that is comparable to that of non-oligotrophic AOB (Kits *et al.*, 2017; Jung *et al.*, 2022).

Ammonia oxidation is an important process in polar soils despite commonly N limited and cold conditions (Alves *et al.*, 2013; Siljanen *et al.*, 2019; Hayashi *et al.*, 2020). AOA generally outnumber AOB in oligotrophic polar soils and are often represented by few species (Alves *et al.*, 2013; Magalhães *et al.*, 2014; Richter *et al.*, 2014; Pessi *et al.*, 2015, 2022, pre-print; Siljanen *et al.*, 2019; Ortiz *et al.*, 2020). Due to their predominance, AOA are important contributors to the N cycle in polar soils and are thus key players in the cycling of the potent greenhouse gas nitrous oxide (N_2O). Contrary to earlier assumptions, polar soils are increasingly recognized as important sources of N_2O (Voigt *et al.*, 2020). Both the nitrite originated from the oxidation of ammonia as well as the nitrate produced in the second step of nitrification are the substrates of denitrification, an anaerobic process that has N_2O as a gaseous intermediate (Butterbach-Bahl *et al.*, 2013). Moreover, AOA have been directly implicated in the production of N_2O under oxic conditions via several mechanisms such as hydroxylalamine oxidation and nitrifier denitrification (Wu *et al.*, 2020). However, both the direct and indirect role of AOA in the cycling of N_2O is much less understood compared to their bacterial counterparts.

AOA are notoriously difficult to cultivate and so far only three genera have been formally described based on axenic cultures: *Nitrosopumilus* (Qin *et al.*, 2017) and *Nitrosarchaeum* (Jung *et al.*, 2018) in the order Nitrosopumilales ("marine group I.1a") and *Nitrososphaera* (Stieglmeier *et al.*, 2014) in the order Nitrososphaerales ("terrestrial group I.1b"). Several provisional *Candidatus* genera have also been proposed based on non-axenic enrichments, e.g. *Ca.* Nitrosocaldus ("termophilic group") (de la Torre *et al.*, 2008) and *Ca.* Nitrosotalea ("group I.1a-associated") (Lehtovirta-Morley *et al.*, 2011). Moreover, the growing use of genome-resolved metagenomics has resulted in the identification of tens of novel, currently uncultured lineages in the phylum Thaumarchaeota (Rinke *et al.*, 2021). These lineages are phylogenetically distinct from both formally described and *Candidatus* taxa and are identified with placeholder alphanumeric identifiers (e.g., the Nitrososphaerales genus "UBA10452"). The identification of these novel lineages by metagenomics greatly expands our knowledge of the diversity of AOA but detailed descriptions of their metabolic and ecological features are generally lacking.

Recently, we have applied a genome-resolved metagenomics approach to gain insights into the microorganisms involved with the cycling of greenhouse gases in tundra soils from Kilpisjärvi, Finland (Pessi *et al.*, 2022, pre-print). Analysis of *amoA* genes encoding the alpha subunit of the enzyme ammonia monooxygenase (Amo) revealed a very low diversity of ammonia oxidizers, with only four genes annotated as *amoA* out of 23.5 million assembled genes. Three of these were most closely related to the *amoA* gene of the comammox bacterium *Ca.* Nitrospira inopinata (Daims *et al.*, 2015). The remaining *amoA* gene was binned into a metagenome-assembled genome (MAG) assigned to the genus "UBA10452", an uncharacterized archaeal lineage in the order Nitrososphaerales, phylum Thaumarchaeota (Rinke *et al.*, 2021). Here, we i) report four novel UBA10452 MAGs obtained from tundra soils in Rásttigáisá, Norway; ii) characterize the genomic properties, metabolic potential, phylogeny, and biogeography of the UBA10452 lineage; and iii) propose the creation of a new *Candidatus* genus, *Ca.* Nitrosopolaris.

Methods

Sampling and metagenome sequencing

Ten soil samples were obtained in July 2017 across an area of alpine tundra in Rásttigáisá, Norway (69°59'N, 26°15'E, 700 m.a.s.l.). DNA was extracted from the mineral layer (10–15 cm depth) with the PowerSoil DNA Isolation kit (QIAGEN, Venlo, Netherlands) according to the manufacturer's instructions. Paired-end metagenomic sequencing was done using the Illumina NextSeq500 platform (Illumina, San Diego, CA, USA) at the DNA Sequencing and Genomics Laboratory (Institute of Biotechnology, University of Helsinki).

Metagenome assembling and binning

Removal of adapter sequences and low-quality base calls (Phred score < 28) was done with Cutadapt v1.10 (Martin, 2011) and sequences were assembled with MEGAHIT v1.1.1 setting a minimum contig length of 1,000 bp (Li *et al.*, 2015). Samples were assembled individually and as one co-assembly of all samples pooled together. Manual MAG binning was done with anvi'o v6.0 (Eren *et al.*, 2015) according to Pessi *et al.* (2022, pre-print). In brief, Prodigal v2.6.3 (Hyatt *et al.*, 2010) was used to predict gene calls and single-copy genes were identified with HMMER v.3.2.1 (Eddy, 2011). Bowtie v2.3.5 (Langmead and Salzberg, 2012) and SAMtools v1.9 (Li *et al.*, 2009) were used to map the quality-filtered Illumina reads to the contigs. Contigs were then manually binned into MAGs based on differential coverage and tetranucleotide frequency using

the *anvi-interactive* interface of anvi'o v6.0. MAGs were manually inspected and refined using the *anvi-refine* interface of anvi'o v6.0.

Metagenome-assembled genomes assigned to the UBA14052 lineage

MAGs were classified based on 122 archaeal and 120 bacterial single-copy genes with GTDB-Tk v1.3.0 (Chaumeil *et al.*, 2019) and the GTDB release 05-RS95 (Parks *et al.*, 2018, 2020). MAGs assigned to the genus "UBA10452" in the order Nitrososphaerales ("terrestrial group I.1b"), phylum Thaumarchaeota (Rinke *et al.*, 2021), were selected for downstream analyses **(Table 1, Suppl. Table S1)**. In addition, we analysed other eight UBA10452 MAGs available on GenBank and GTDB release 95 (Parks *et al.*, 2018, 2020). These included six MAGs from permafrost soil in Canada (Chauhan *et al.*, 2014; Parks *et al.*, 2017), one MAG from polar desert soil in Antarctica (Ji *et al.*, 2017), and one MAG from tundra soil in Finland (Pessi *et al.*, 2022).

Genome annotation

We used anvi'o v7.0 (Eren *et al.*, 2015) to predict gene calls with Prodigal v2.6.3 (Hyatt *et al.*, 2010), identify ribosomal genes and a set of 76 archaeal single-copy genes with HMMER v.3.3 (Eddy, 2011), and compute genome completion and redundancy levels based on the presence of the 76 single-copy genes. We also employed anvi'o v7.0 to annotate the gene calls against the KOfam (Aramaki *et al.*, 2020) and Pfam (Mistry *et al.*, 2021) databases with HMMER v.3.3 (Eddy, 2011) and the COG database (Galperin *et al.*, 2021) with DIAMOND v0.9.14 (Buchfink *et al.*, 2015). Additionally, we used BLASTP v2.10.1 (Camacho *et al.*, 2009) to annotate the gene calls against the arCOG database (Makarova *et al.*, 2015). Matches with scores below the pre-computed family-specific thresholds (KOfam and Pfam), e-value > 10^{-6} (COG), or identity < 35% and coverage < 75% (arCOG) were discarded and, in case of multiple matches, the one with the lowest e-value was kept.

We used BLASTP v2.10.1 to compare the amino acid sequences of genes identified as *amoA*, *amoB*, or *amoC* to the RefSeq (O'Leary *et al.*, 2016) and Swiss-Prot (The UniProt Consortium, 2019) databases, and BLASTN v2.10.1 (Camacho *et al.*, 2009) to compare *amoA* genes against the nt database and the curated *amoA* database of Alves *et al.* (2018). Functional enrichment analyses were carried out using anvi'o v7.0 (Eren *et al.*, 2015) according to Shaiber *et al.* (2020). In brief, the occurrence of arCOG functions across genomes was summarised and logistic regression was then used to identify functions associated with a particular genus or genera. For this, we considered only the three most complete *Nitrososphaera*, *Ca.* Nitrosocosmicus, and *Ca.* Nitrosodeserticola genomes plus the representative genome of each *Ca.* Nitrosopolaris species.

126 **Table 1.** List of metagenome-assembled genomes (MAGs) belonging to the UBA10452 lineage
127 (*Candidatus* Nitrosopolaris).

128 MAG	Isolation source	Accession	Ref.
129 COA_Bin_4_1	Tundra soil, Rásttigáisá, Norway	GCA_933227015.1	[1]
130 S89_Bin_2	Tundra soil, Rásttigáisá, Norway	GCA_933227005.1	[1]
131 S100_Bin_4	Tundra soil, Rásttigáisá, Norway	GCA_933226995.1	[1]
132 S1130_Bin_3	Tundra soil, Rásttigáisá, Norway	GCA_933226985.1	[1]
133 KWL-0179	Tundra soil, Kilpisjärvi, Finland	GCA_936417005.1	[2]
134 UBA272	Permafrost soil, Nunavut, Canada	GCA_002504425.1	[3]
135 UBA273	Permafrost soil, Nunavut, Canada	GCA_002501935.1	[3]
136 UBA347	Permafrost soil (active layer), Nunavut, Canada	GCA_002495965.1	[3]
137 UBA348	Permafrost soil (active layer), Nunavut, Canada	GCA_002501855.1	[3]
138 UBA466	Permafrost soil (active layer), Nunavut, Canada	GCA_002498345.1	[3]
139 UBA536	Permafrost soil (active layer), Nunavut, Canada	GCA_002496625.1	[3]
140 RRmetagenome_bin19	Polar desert soil, Wilkes Land, Antarctica	GCA_003176995.1	[4]

141 1. This study.
142 2. Pessi et al. (2022, pre-print).
143 3. Parks et al. (2017), based on data originally published by Chauhan et al. (2014).
144 4. Ji et al. (2017).

145 Phylogenomic and phylogenetic analyses

146 For phylogenomic analysis, we used a set of 59 archaeal single-copy genes that were present in
147 at least 80% of the genomes. In addition to the 12 UBA10452 MAGs, we retrieved from GenBank
148 other 33 genomes belonging to the family Nitrososphaeraceae and the genome of
149 *Nitrosopumilus maritimus* SCM1 to be used as an outgroup. We used anvi'o v7.0 (Eren *et al.*,
150 2015) to recover the predicted amino acid sequence for each of the 59 genes, align them
151 individually with MUSCLE v3.8.1551 (Edgar, 2004), and generate a concatenated alignment.
152 We then computed a maximum likelihood tree with IQ-TREE v2.1.4 employing the automatic
153 model selection and 1000 bootstraps (Nguyen *et al.*, 2015). Pairwise average nucleotide identity
154 (ANI) values were computed with pyani v0.2.10 (Pritchard *et al.*, 2016) and amino acid identity
155 (AAI) values with the AAI-Matrix tool (http://enve-omics.ce.gatech.edu/g-matrix).

156 Phylogenetic analysis of the *amoA* and 16S rRNA genes were done as described for the
157 phylogenomic analysis (i.e., alignment with MUSCLE and tree building with IQ-TREE). Genes
158 annotated as multicopper oxidase (PF07731, PF07732, COG2132, or arCOG03914) or nitrite
159 reductase were aligned with MAFFT v7.490 (Katoh and Standley, 2013) alongside the

sequences reported by Kerou *et al.* (2016), and a maximum likelihood tree was computed with IQ-TREE v2.1.4 (Nguyen *et al.*, 2015) as described above.

Abundance and geographic distribution

We employed read recruitment to compute the relative abundance of the UBA10452 lineage across the metagenomics datasets from which the MAGs were originally recovered. These datasets consisted of 10 Illumina NextSeq metagenomes from tundra soils in Rásttigáisá, Norway (this study); 69 Illumina NextSeq/NovaSeq metagenomes from tundra soils in Kilpisjärvi, Finland (Pessi *et al.*, 2022, pre-print); 13 Illumina HiSeq metagenomes from permafrost soils in Nunavut, Canada (Chauhan *et al.*, 2014; Stackhouse *et al.*, 2015); and three Illumina HiSeq metagenomes from polar desert soils in Wilkes Land, Antarctica (Ji *et al.*, 2017). We used fasterq-dump v2.10.8 (https://github.com/ncbi/sra-tools) to retrieve the raw metagenomic data from the Sequence Read Archive (SRA). We then used CoverM v0.6.1 (https://github.com/wwood/CoverM) to map the reads to the MAGs with minimap v2.17 (Li, 2016) and to compute relative abundances based on the proportion of reads recruited by the MAGs. In addition, we used IMNGS (Lagkouvardos *et al.*, 2016) to further investigate the geographic distribution of the UBA10452 lineage. For this, we used the 16S rRNA gene sequence of the MAG RRmetagenome_bin19 as query to screen 422,877 amplicon sequencing datasets in SRA with UBLAST (Edgar, 2010). We considered only matches with ≥ 99.0% similarity.

Results

Genomic characteristics of the UBA10452 lineage

We applied a genome-resolved metagenomics approach to data obtained from tundra soils in Rásttigáisá, Norway, and recovered four MAGs assigned to the genus "UBA10452", an uncultured lineage in the order Nitrososphaerales ("terrestrial group I.1b"), phylum Thaumarchaeota (Rinke *et al.*, 2021). The UBA10452 lineage is currently represented by eight MAGs in GTDB and GenBank in addition to the four MAGs obtained in the present study **(Table 1, Fig. 1a)**. Genome completion and redundancy estimated with anvi'o v7.0 (Eren *et al.*, 2015) based on the presence of 76 single-copy genes range from 50.0–90.8% and 2.6–9.2%, respectively **(Fig. 1b, Suppl. Table S1)**. The MAG RRmetagenome_bin19, with 90.8% completion, 3.9% redundancy, and a nearly complete (1462 bp) 16S rRNA gene, is a high-quality MAG according to the MIMAG standard (Bowers *et al.*, 2017). The remaining 11 MAGs are of medium quality (≥ 50% complete, < 10% redundant), four of which also include the 16S rRNA

191 gene. The genome size of UBA10452 MAGs ranges from 0.8 Mb (MAG S1130_Bin_3, 60.5%
192 complete) to 4.0 Mb (MAG RRmetagenome_bin19, 90.8% complete). G+C content ranges from
193 38.1 to 41.5%.

194 UBA10452 has a predominantly polar distribution

195 All 12 UBA10452 MAGs were obtained from tundra, permafrost, and polar desert soils **(Table**
196 **1, Fig. 1a)**. To gain insights into the ecology of the UBA10452 lineage, we used read recruitment
197 to quantify the abundance of UBA10452 MAGs in the metagenomic datasets from which they
198 were assembled. UBA10452 MAGs were most abundant in the dataset of permafrost from
199 nutrient-poor (C: 1.0%, N: 0.1%) mineral cryosoils in Nunavut, Canadian Arctic, where they
200 recruited up to 8.6% of the reads in each sample **(Fig. 1c)**. On the other hand, UBA10452 MAGs
201 were least abundant in the more nutrient-rich (C: 7.3%, N: 0.3%) tundra soils from Kilpisjärvi,
202 Finland, where they were detected particularly in samples taken from the mineral layer of
203 heathland and meadow soils.

204 In order to investigate further the geographic distribution of the UBA10452 lineage, we used
205 IMNGS (Lagkouvardos *et al.*, 2016) to screen 422,877 16S rRNA gene amplicon sequencing
206 datasets in SRA. Sequences matching the 16S rRNA gene of UBA10452 MAGs (≥ 99.0%
207 similarity) were found across 1281 datasets, mostly consisting of soil (n = 750), freshwater (n =
208 104), and rhizosphere samples (n = 100). Matched reads accounted for 6.0% of the total number
209 of reads in these datasets (8.9 out of 149.1 million sequences). Of these, the overwhelming
210 majority (8.7 million reads, 97.9%) come from Antarctic soil datasets, particularly from 149 sites
211 in the vicinity of Davis Station, Princess Elizabeth Land (Bissett *et al.*, 2016) **(Suppl. Fig. S1a)**.
212 The proportion of reads matching the UBA10452 lineage was above 50% of the archaeal 16S
213 rRNA gene sequences in 70 of these sites and reached values as high as 88.8% **(Suppl. Fig.**
214 **S1b)**.

215 UBA10452 is a distinct lineage in the family Nitrososphaeraceae

216 Phylogenomic analysis based on 59 single2-copy genes placed the UBA10452 MAGs as a distinct
217 lineage outside *Nitrososphaera*, *Ca.* Nitrosocosmicus, and *Ca.* Nitrosodeserticola, the three
218 described genera in the family Nitrososphaeraceae (Stieglmeier *et al.*, 2014; Lehtovirta-Morley
219 *et al.*, 2016; Hwang *et al.*, 2021) **(Fig. 2a; Suppl. Fig. S2)**. Separation of UBA10452 is also
220 supported by AAI and 16S rRNA gene analyses. UBA10452 MAGs share 59.1% ± 1.9, 53.0% ±
221 1.1, and 53.8% ± 0.9 AAI with *Nitrososphaera*, *Ca.* Nitrosocosmicus, and *Ca.* Nitrosodeserticola,
222 respectively **(Fig. 2b)**, all of which are below the 65% AAI threshold commonly used to delineate

microbial genera (Konstantinidis *et al.*, 2017). At the 16S rRNA gene level, UBA10452 MAGs are 94.8% ± 1.2 and 95.4% ± 0.2 similar to *Nitrososphaera* and *Ca*. Nitrosocosmicus, respectively **(Suppl. Fig. S3)**. These values are in the limit of the 95% threshold for genus delineation proposed by Rosselló-Móra and Amann (2015), but are well below the median 16S rRNA gene similarity observed between related genera across different microbial phyla (96.4%; Yarza *et al.*, 2014). Comparison with *Ca*. Nitrosodeserticola was not possible due to the lack of a 16S rRNA gene sequence from this genus. Given that UBA10452 represents a clear, distinct lineage in the family Nitrososphaeraceae, we consider that UBA10452 should be recognized as a *Candidatus* genus and propose the name *Ca*. Nitrosopolaris.

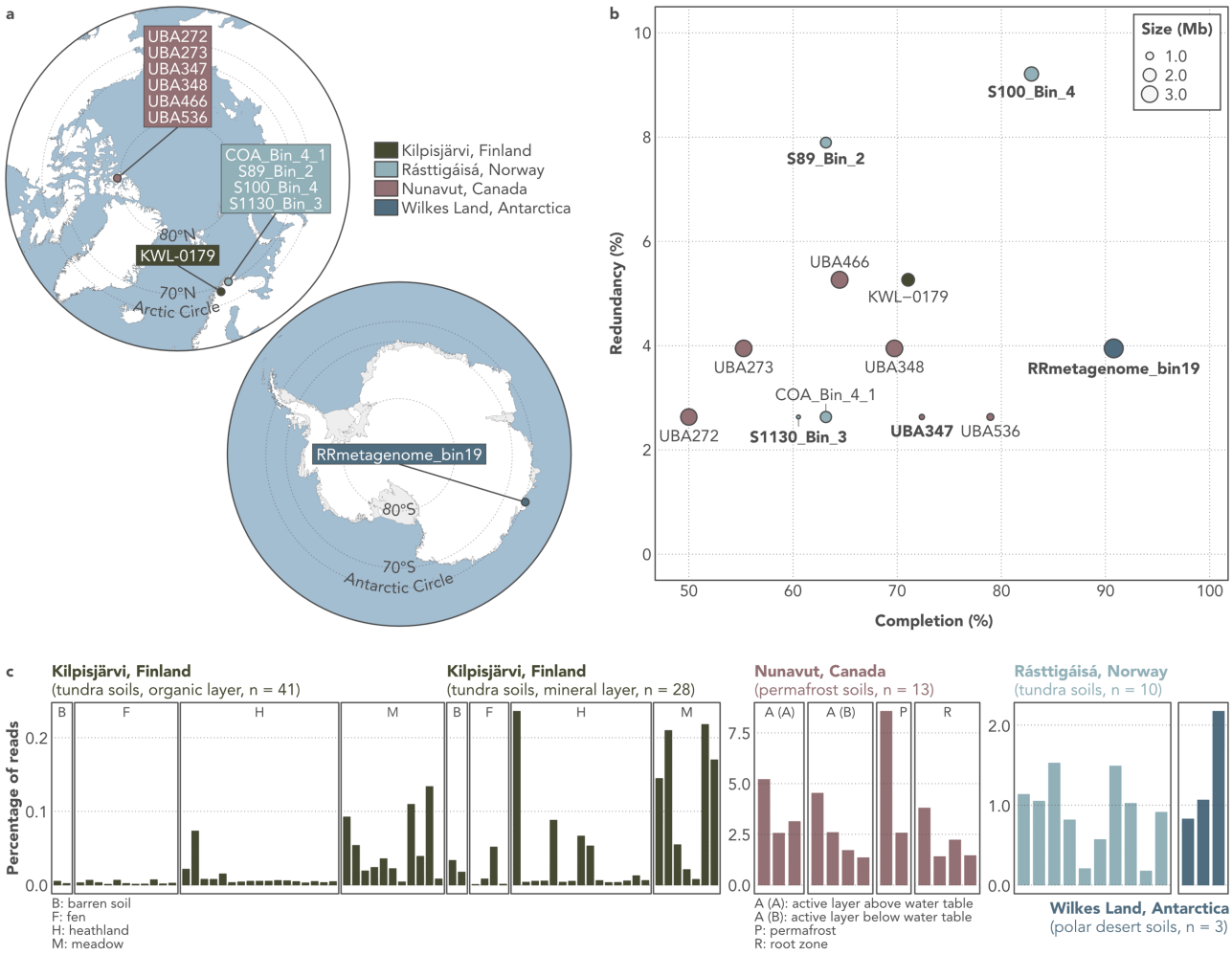

Figure 1. Geographic origin, assembly statistics, and abundance of metagenome-assembled genomes (MAGs) assigned to the UBA10452 lineage (*Candidatus* Nitrosopolaris). a) Maps of the Arctic and Antarctic regions showing the geographic origin of the 12 UBA10452 MAGs. **b)** Genome completion, redundancy, and size of the UBA10452 MAGs. Completion and redundancy levels were computed based on the presence of 76 single-copy genes. MAGs in bold include the 16S rRNA gene. **c)** Proportion of metagenomic reads recruited by the UBA10452 MAGs across the four datasets from which they were originally recovered.

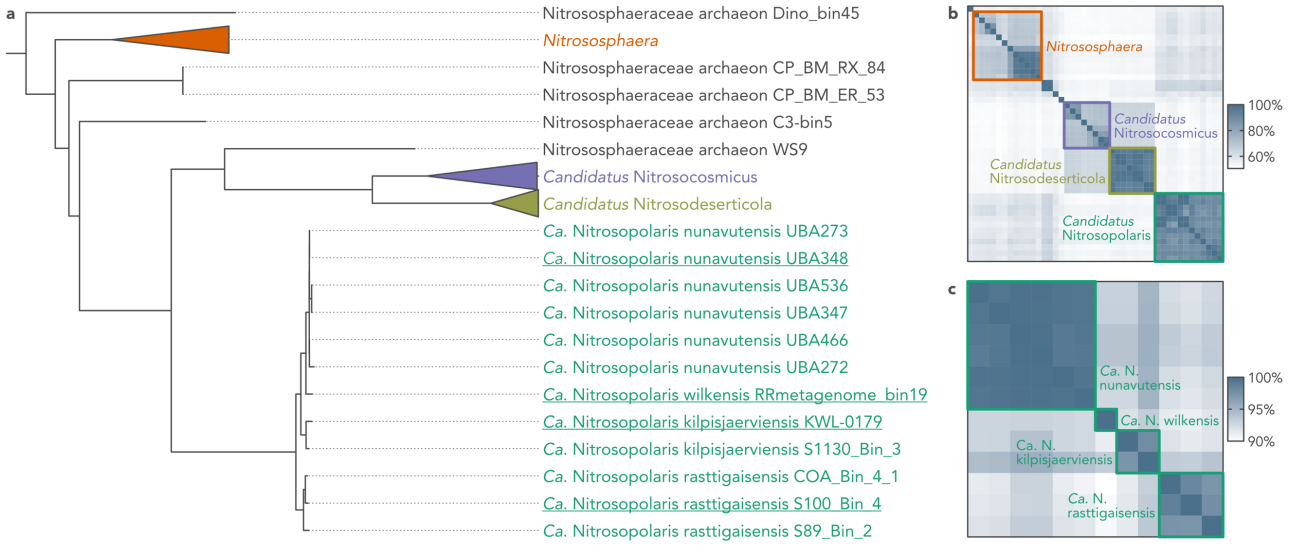

Figure 2. Phylogenomic analysis of the UBA10452 lineage (*Candidatus* Nitrosopolaris). a) Maximum likelihood tree based on 59 single-copy genes from 12 metagenome-assembled genomes (MAGs) assigned to the UBA10452 lineage and 33 other Nitrososphaeraceae genomes available on GenBank. The tree was rooted with *Nitrosopumilus maritimus* SCM1 (not shown). Representatives for the four proposed species are indicated in underscore. An uncollapsed and bootstrapped version of the tree can be found in **Suppl. Fig. S2**. **b)** Pairwise average amino acid identity (AAI) between Nitrososphaeraceae genomes and **c)** average nucleotide identity (ANI) between UBA10452 MAGs. The boxes encompass the four described Nitrososphaeraceae genera (AAI threshold of 65%; panel b) and the four proposed species of *Candidatus* Nitrosopolaris (ANI threshold of 95–96%; panel c). Rows and columns are ordered from top to bottom and left to right, respectively, according to the top-bottom order of leaves in panel a.

Pairwise ANI values between *Ca.* Nitrosopolaris MAGs range from 90.9 to 99.9% **(Fig. 2c)**. Based on either a 95% (Konstantinidis *et al.*, 2017) or 96% ANI threshold (Ciufo *et al.*, 2018), the 12 *Ca.* Nitrosopolaris MAGs can be separated into four distinct species **(Fig. 2a; Suppl. Fig. S2)**. Two of these, one comprising the six Canadian MAGs (Chauhan *et al.*, 2014; Parks *et al.*, 2017) and the other consisting solely of the Antarctic MAG (Ji *et al.*, 2017), correspond to the two existing species in GTDB release 95 ("UBA10452 sp002501855" and "UBA10452 sp003176995", respectively). Here we suggest renaming these species as *Ca.* Nitrosopolaris nunavutensis and *Ca.* Nitrosopolaris wilkensis, respectively, according to the geographic origin of the MAGs. The Finnish MAG (Pessi *et al.*, 2022, pre-print) plus one of the Norwegian MAGs obtained in the present study (S1130_Bin_3) represent a novel species, for which we suggest the name *Ca.* Nitrosopolaris kilpisjaerviensis. Finally, the three remaining MAGs obtained in the present study (COA_Bin_4_1, S89_Bin_2, and S100_Bin_4) correspond to another novel species, which we propose to be named as *Ca.* Nitrosopolaris rasttigaisensis. However, the separation of *Ca.* Nitrosopolaris into four species is not supported by the analysis of the 16S rRNA gene **(Suppl. Fig. S3)**. The pairwise similarity between 16S rRNA gene sequences across the four

264 ANI clusters range from 99.5 to 99.9%, which is above the 98.7–99.0% threshold commonly used
265 for species delineation (Stackebrandt and Ebers, 2006; Kim *et al.*, 2014).

266 *Ca.* Nitrosopolaris harbours genes for ammonia oxidation, CO_2 fixation, and 267 carbohydrate metabolism and transport

268 Annotation of protein-coding genes revealed that *Ca.* Nitrosopolaris harbours the *amoA*, *amoB*,
269 *amoC*, and *amoX* genes encoding the enzyme ammonia monooxygenase (Amo) which catalyses
270 the oxidation of ammonia to hydroxylamine **(Fig. 3a, Suppl. Fig. S4, Suppl. Table S2)**. As for
271 other AOA, homologues of the *hao* gene were not found in the *Ca.* Nitrosopolaris MAGs. In AOB,
272 this gene encodes the enzyme hydroxylamine dehydrogenase (Hao) which takes part in the
273 oxidation of hydroxylamine to nitrite, a mechanism that remains unknown in AOA (Lehtovirta-
274 Morley, 2018). A proposed mechanism of hydroxylamine oxidation in AOA is via a copper-
275 containing nitrite reductase (NirK) encoded by the *nirK* gene, which has been detected in most
276 *Ca.* Nitrosopolaris MAGs as well as other related multicopper oxidases **(Suppl. Fig. S4)**. *Ca.*
277 Nitrosopolaris also encodes an ammonium transporter of the Amt family involved in the uptake
278 of extracellular ammonium. Moreover, *Ca.* Nitrosopolaris harbours urease (*ureABC*) and urea
279 transporter (*utp*) genes, indicating the ability to generate ammonia from urea. In contrast to
280 *Nitrososphaera gargensis* (Spang *et al.*, 2012), we did not detect the *cynS* gene encoding the
281 enzyme cyanate hydratase involved in the production of ammonia from cyanate.

282 The *amo* genes in all *Ca.* Nitrosopolaris MAGs are distributed across two separate contigs **(Fig.**
283 **3a)**. One of the contigs contains the *amoC*, *amoX*, and *amoA* genes; however, the *amoC* gene is
284 truncated and found in only two MAGs. In some MAGs, the other contig contains a second, full-
285 length copy of the *amoC* gene followed by *amoB*. Not all MAGs contain all *amoABCX* genes.
286 However, considering that the MAGs present varying levels of completion **(Fig. 1b, Suppl.**
287 **Table S1)** and since the localization of the genes corresponds to start or end of contigs **(Fig.**
288 **3a)**, it is likely that missing genes are an artifact of truncated assemblies rather than due to
289 gene loss. The *amoA* gene of *Ca.* Nitrosopolaris has a length of 651 bp and belongs to the NS-γ-
290 2.3.2 cluster of Alves *et al.* (2018) **(Fig. 3b)**. One exception is the MAG UBA272 which contains
291 a longer *amoA* gene (873 bp) with a long insert of ambiguous base calls, most likely an artifact
292 from assembling and/or scaffolding. Sequences belonging to the NS-γ-2.3.2 cluster are found
293 majorly in acidic soils (Alves *et al.*, 2018). Moreover, analysis of sequences from GenBank
294 showed that the *amoA* gene of *Ca.* Nitrosopolaris is related (≥ 96% nucleotide similarity) to
295 sequences recovered mostly from cold environments, i.e., the Artic, Antarctica, and alpine
296 regions such as the Tibetan Plateau **(Fig. 3c)**. Among these, the *amoA* sequences of *Ca.*

Nitrosopolaris MAGs are most closely related (98.9–99.7% nucleotide similarity) to uncultured sequences from Antarctic soil (MH318339 and MH318307), grassland soil in Iceland (JQ403917 and JQ403913), and the Tibetan Plateau (GQ143258, GQ143220, GQ143135, KF004058, and MK987234) (Daebeler *et al.*, 2012; Xie *et al.*, 2014; Wang *et al.*, 2019; Zhang *et al.*, 2019) **(Fig. 3b)**.

Similarly to other AOA, *Ca.* Nitrosopolaris harbours genes for the hydroxypropionate-hydroxybutyrate pathway of CO_2 fixation, complexes I–V of the electron transfer chain, the citric acid cycle, and gluconeogenesis **(Suppl. Fig. S4, Suppl. Table S2)**. Like other AOA, the gene content of *Ca.* Nitrosopolaris indicates a potential for mixotrophic metabolism, with multiple copies of genes encoding proteins involved in carbohydrate metabolism and transport such as glucose/sorbosone dehydrogenases, permeases of the major facilitator superfamily (MFS), and pyruvate oxidases. In contrast to *Nitrososphaera*, we did not detect genes involved in the assembly of pili, flagellar apparatus (archaellum), and chemotaxis.

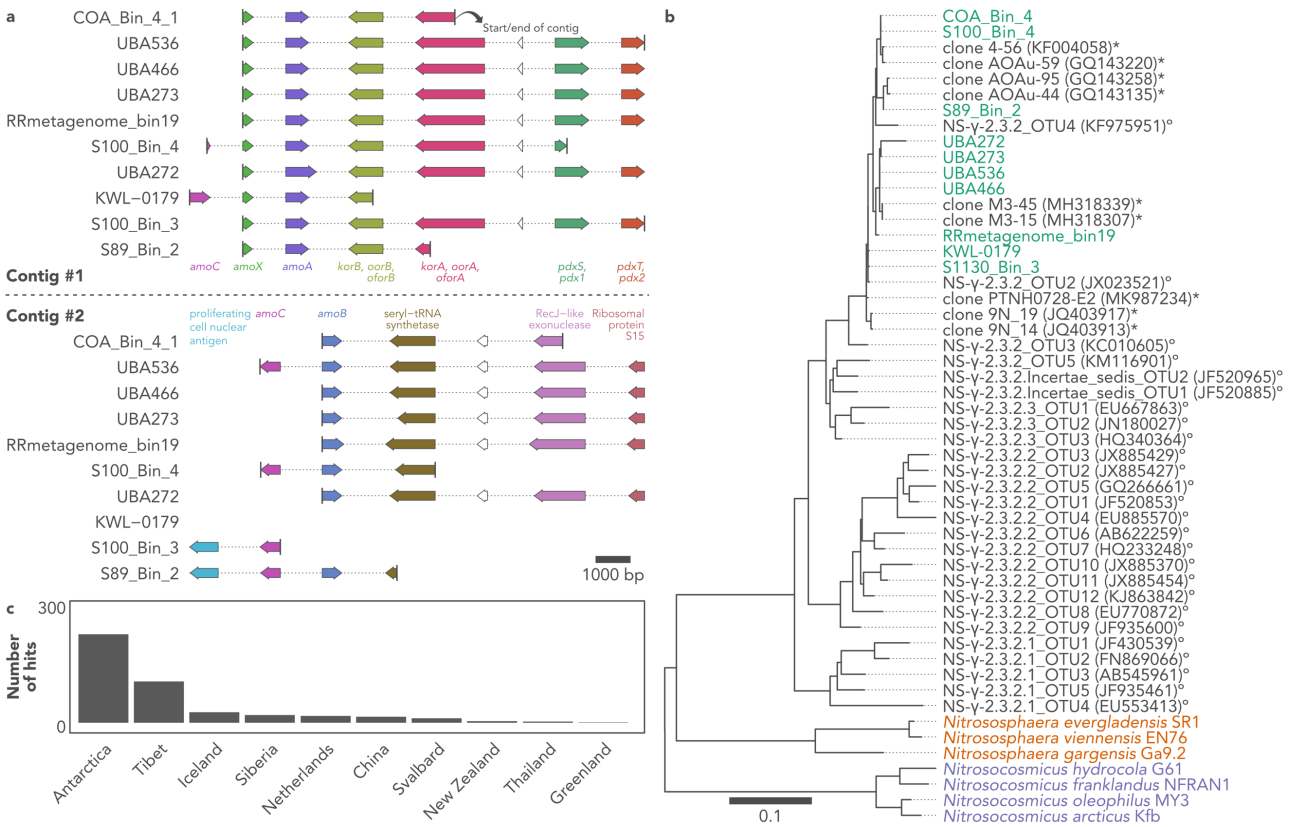

Figure 3. The ammonia monooxygenase (*amo*) genes of UBA10452 (*Candidatus* Nitrosopolaris). a) Representation of two contigs containing *amo* genes in metagenome-assembled genomes (MAGs) assigned to the UBA10452 lineage. Two MAGs which do not contain the *amoA* gene are omitted (UBA347 and UBA348). **b)** Maximum likelihood tree of the *amoA* sequence of UBA10452 MAGs and related sequences from GenBank (asterisks) and Alves *et al.* (2018) (circles). **c)** Geographic origin of sequences from GenBank with ≥ 96.0% nucleotide similarity to the *amoA* sequence of UBA10452 MAGs.

317 ## *Ca.* Nitrosopolaris MAGs are enriched in genes involved in DNA replication
318 and repair

319 To investigate possible mechanisms underlying the distribution of *Ca.* Nitrosopolaris, we
320 carried out a functional enrichment analysis covering the four Nitrososphaeraceae genera. In
321 total, the 13 MAGs used in the analysis encoded 3,999 different arCOG functions **(Fig. 4a)**. Of
322 these, 948 functions were shared among all four genera and 368 were unique to *Ca.*
323 Nitrosopolaris. Of the arCOG functions shared by all four genera, most belonged to the arCOG
324 classes translation, ribosomal structure, and biogenesis (n = 114), function unknown (n = 88),
325 and amino acid transport and metabolism (n = 73). On the other hand, arCOG functions unique
326 to *Ca.* Nitrosopolaris belonged mostly to the arCOG classes function unknown (n = 59), general
327 function prediction only (n = 52), and inorganic ion transport and metabolism (n = 33). Among
328 these arCOG functions are several types of hydrolases, lipoproteins, phospholipases, and ABC
329 transporters including ones for iron, maltose, phosphate, amino acids, and nucleosides **(Suppl.**
330 **Table S3)**.

331 In addition to the genome-wide functional enrichment analysis, we also looked more specifically
332 for genes with known or predicted roles in cold adaptation and growth (Raymond-Bouchard *et*
333 *al.*, 2018). When comparing the genomic repertoire of *Ca.* Nitrosopolaris to the other
334 Nitrososphaeraceae genera, the former was found to harbour a higher number of genes involved
335 in DNA replication and repair **(Fig. 4b)**. More specifically, *Ca.* Nitrosopolaris MAGs encode
336 multiple copies of the enzymes RecA ATPases and RecA/RadA recombinases **(Suppl. Table S4)**.
337 Surprisingly, genes related to cold shock response were less abundant in *Ca.* Nitrosopolaris
338 compared to *Nitrososphaera* and *Ca.* Nitrosocosmicus **(Fig. 4b)**, although several copies of
339 molecular chaperones (DnaK, GrpE, and IbpA) and universal stress proteins (UspA) were
340 identified **(Suppl. Table S4)**. In addition to these, *Ca.* Nitrosopolaris also harbours several
341 copies of other genes encoding proteins related to cold adaptation and growth **(Fig. 4b)**,
342 including proteins involved in membrane and peptidoglycan alteration (glycosyltransferases),
343 osmotic stress (sodium-hydrogen antiporters and sodium-proline symporters), oxidative stress
344 (periredoxins and thioredoxin reductases), and translation/transcription (DNA/RNA helicases
345 and transcription factors) **(Suppl. Table S4)**.

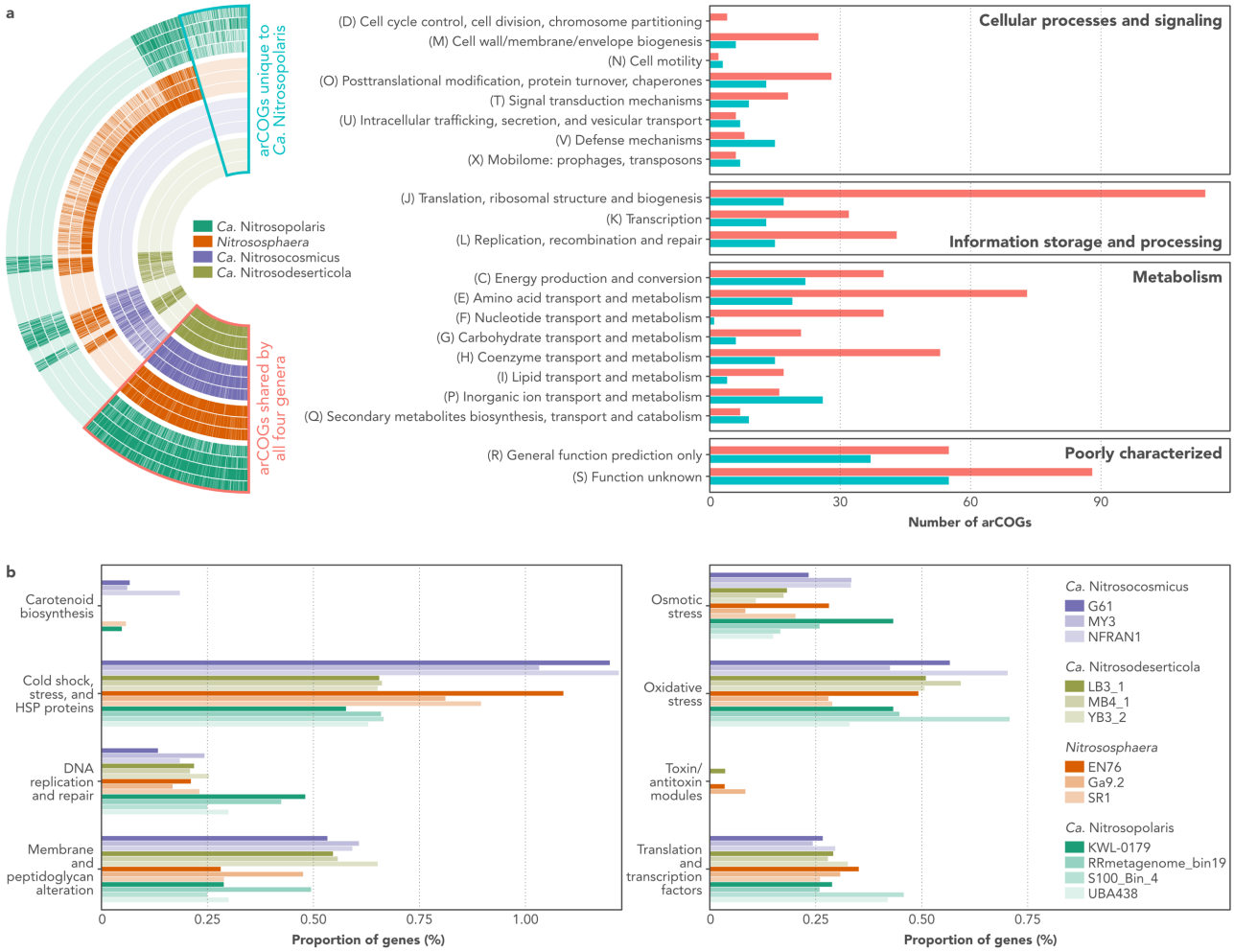

Figure 4. Comparative genomics of the UBA10452 lineage (*Candidatus* Nitrosopolaris) and other members of the family Nitrososphaeraceae. a) Functional enrichment analysis showing arCOG functions shared by all Nitrososphaeraceae genera and other functions unique to *Ca.* Nitrosopolaris. More detail on the arCOG functions unique to *Ca.* Nitrosopolaris can be found in **Suppl. Table S3**. **b)** Distribution of genes with known or predicted roles in cold adaptation and growth (Raymond-Bouchard *et al.*, 2018). Number of genes is shown as a proportion of the total number of genes in each genome. More detail on the genes found in *Ca.* Nitrosopolaris can be found in **Suppl. Table S4**.

Discussion

Genome-resolved metagenomics has revolutionized our knowledge of archaeal diversity by giving us access to the genome of uncultured microorganisms at an unprecedented rate (Tahon *et al.*, 2021). In a recent metagenomic investigation of tundra soils in northern Finland (Pessi *et al.*, 2022, pre-print), we have manually binned and curated a MAG belonging to the genus "UBA10452", an uncultured and largely uncharacterized lineage in the order Nitrososphaerales ("terrestrial group I.1b") of the phylum Thaumarchaeota (Rinke *et al.*, 2021). Here, we binned four other UBA10452 MAGs from tundra soils in Rásttigáisá, Norway, and characterized the phylogeny, metabolic potential, and biogeography of this lineage. Our results indicate that the

363 UBA10452 lineage consists of putative AOA with a geographic distribution mostly restricted to
364 cold ecosystems, particularly the polar regions. We suggest the recognition of UBA10452 as a
365 *Candidatus* genus, for which we propose the name *Ca.* Nitrosopolaris (*nitrosus*: Latin adjective
366 meaning nitrous; *polaris*: Latin adjective meaning of or pertaining to the poles).

367 The findings from our polyphasic analysis consisting of phylogenomic, AAI, and 16S rRNA gene
368 analyses support the placement of *Ca.* Nitrosopolaris outside *Nitrososphaera*, *Ca.*
369 Nitrosocosmicus, and *Ca.* Nitrosodeserticola in the family Nitrososphaeraceae, as previously
370 suggested (Rinke *et al.*, 2021). Our results further indicate that the 12 *Ca.* Nitrosopolaris MAGs
371 represent four different species based on a 95–96% ANI threshold (Konstantinidis *et al.*, 2017;
372 Ciufo *et al.*, 2018). In addition to the two current species in GTDB release 95 (Parks *et al.*, 2018,
373 2020), the inclusion of the four MAGs obtained in the present study resulted in the identification
374 of two novel species. It is important to note that the separation of *Ca.* Nitrosopolaris into four
375 species based on ANI values is not readily supported by the analysis of 16S rRNA gene
376 sequences, which are ≥ 99.5% similar across the four species. Although a 98.7–99.0% threshold
377 is commonly used (Stackebrandt and Ebers, 2006), species delineation based solely on the 16S
378 rRNA gene can be problematic given that microorganisms belonging to different species can
379 share identical 16S rRNA gene sequences (Kim *et al.*, 2014; Schloss, 2021). One example of this
380 is *Ca.* Nitrosocosmicus arcticus and *Ca.* Nitrosocosmicus oleophilus, two species of AOA which
381 share an identical 16S rRNA gene sequence despite having divergent genomes with only 83.0%
382 ANI (Alves *et al.*, 2019). It thus appears reasonable to conclude that the 12 *Ca.* Nitrosopolaris
383 MAGs indeed represent four different species as suggested by the ANI analysis. If cultured
384 representatives become available in the future, phenotypic and ecophysiological
385 characterization of these isolates could help resolve the taxonomy of *Ca.* Nitrosopolaris.

386 *Ca.* Nitrosopolaris harbours the complete set of *amoA* genes responsible for chemolithotrophic
387 growth via ammonia oxidation (Lehtovirta-Morley, 2018). Although *in silico* analyses provide
388 valuable predictions, metabolic capabilities inferred by genomic annotation need to be
389 confirmed based on the analysis of isolated/enriched cultures or with the help of other indirect
390 methods such as stable isotope probing (SIP) (Gadkari *et al.*, 2020). Nevertheless, the putative
391 ammonia oxidation capability of *Ca.* Nitrosopolaris is supported by its close phylogenetic
392 relationship to *Nitrososphaera* and *Ca.* Nitrosocosmicus, two genera which have been
393 demonstrated to grow by oxidizing ammonia (Stieglmeier *et al.*, 2014; Lehtovirta-Morley *et al.*,
394 2016). In addition, the presence of several genes involved in carbohydrate and amino acid
395 transport and metabolism suggest that *Ca.* Nitrosopolaris, like other AOA, might be able to
396 grow mixotrophically using organic compounds as alternative energy and/or C sources
397 (Mussmann *et al.*, 2011; Pester *et al.*, 2011).

398 In addition to the geographical origin of the MAGs, large-scale screening of 16S rRNA gene and
399 *amoA* sequences from SRA and GenBank indicate that *Ca.* Nitrosopolaris is restricted to soils
400 in the cold biosphere. The soils from which the *Ca.* Nitrosopolaris MAGs have been recovered
401 are typical of polar and alpine environments, being characterized by low pH (4.8–5.1), carbon
402 (C) (1.0–7.3%), and N (0.1–0.3%) content (Stackhouse *et al.*, 2015; Ji *et al.*, 2017; Pessi *et al.*,
403 2022, pre-print). Furthermore, the abundance profile of *Ca.* Nitrosopolaris observed in this
404 study, which was characterized by a higher abundance in mineral cryosoil permafrost and polar
405 desert soils compared to vegetated tundra soils, indicates that *Ca.* Nitrosopolaris is particularly
406 adapted to the highly oligotrophic conditions found in some of the most extreme environments
407 in the cryosphere. The discovery of *Ca.* Nitrosopolaris complements the list of microbial taxa
408 that appear to be adapted to life in cold environments, such as the mat-forming cyanobacteria
409 *Phormidesmis priestleyi* (Komárek *et al.*, 2009) and *Shackeltoniella antarctica* (Strunecky *et al.*,
410 2020) and the sea-ice bacteria *Polaribacter* and *Psychrobacter* (Bowman, 2013).

411 Investigation of the genome of *Ca.* Nitrosopolaris provided insights on possible adaptations to
412 cold and oligotrophic environments. For instance, *Ca.* Nitrosopolaris harbour multiple copies of
413 several genes that have been implicated in tolerance to cold, such as genes encoding proteins
414 involved in DNA replication and repair, molecular chaperones, DNA/RNA helicases, and
415 universal stress proteins (Raymond-Bouchard *et al.*, 2018). Interestingly, *Ca.* Nitrosopolaris
416 appears to be enriched in copies of the RecA enzyme compared to other members of the
417 Nitrososphaeraceae. RecA plays a key role in DNA repair, which is an important mechanism
418 for survival in polar environments where DNA is frequently damaged due to freezing and UV
419 radiation (Cavicchioli, 2006). In addition to the possible adaptive mechanisms of *Ca.*
420 Nitrosopolaris, it has been suggested that the environmental characteristics of polar soils favour
421 AOA in general (Alves *et al.*, 2013; Siljanen *et al.*, 2019). The ecological success of AOA in
422 oligotrophic and acidic soils has been traditionally linked to the higher affinity of their ammonia
423 oxidation machinery compared to their bacterial counterparts (Martens-Habbena *et al.*, 2009;
424 Kerou *et al.*, 2016), although a recent study has shown that high affinity for ammonia is not
425 common to all AOA (Jung *et al.*, 2022). Furthermore, the hydroxypropionate-hydroxybutylate
426 pathway of CO_2 fixation encoded by *Ca.* Nitrosopolaris and other AOA appears to be more
427 energy efficient than the Calvin cycle employed by AOB (Könneke *et al.*, 2014). However, these
428 traits are shared between *Ca.* Nitrosopolaris and other AOA and thus do not readily explain the
429 apparent ecological success of *Ca.* Nitrosopolaris in cold environments. Indeed, mechanisms of
430 cold adaptation are evolutionary and functionally complex and involve many features that
431 cannot be observed by metagenomics alone (e.g., gene regulation and membrane modifications)

(Cavicchioli, 2006). Structural, transcriptomics, and proteomics analysis of cultured isolates could help shed further light on possible adaptations to cold in *Ca.* Nitrosopolaris.

In addition to possible mechanisms of adaptation to polar environments, we hypothesize that the distribution of *Ca.* Nitrosopolaris could be, to some extent, related to historical factors. Interestingly, the four proposed *Ca.* Nitrosopolaris species form coherent biogeographical clusters: *Ca.* N. nunavutensis, comprising MAGs obtained from permafrost soils in Nunavut, Canada; *Ca.* N. wilkensis, corresponding to one MAG from polar desert soils in Wilkes Land, Antarctica; and *Ca.* N. kilpisjaerviensis and *Ca.* N. rasttigaisensis, comprising MAGs obtained from mineral tundra soils in two relatively close regions in northern Fennoscandia (Kilpisjärvi and Rásttigáisá, respectively). A recent molecular dating study has suggested that the origin of the AOA clade group I.1b (order Nitrososphaerales) coincides with severe glaciation events that happened during the Neoproterozoic (Yang *et al.*, 2021). If these estimates are accurate, it would imply that *Ca.* Nitrosopolaris and all other lineages in group I.1b share a common ancestor that appeared when the global climate was characterized by sub-zero temperatures, having likely evolved at glacial refugia such as nunataks or regions with geothermal activity.

Due to low temperatures throughout the year, polar soils store a large amount of organic matter and have thus served as important carbon sinks. At present, polar soils are considered minor yet significant sources of N_2O (Voigt *et al.*, 2020) but, if warming trends continue at the levels observed currently, polar soils might become major contributors to the global N_2O budget. For instance, the AOA *Ca.* Nitrosocosmicus arcticus isolated from Arctic soil has an ammonia oxidation optimum at temperatures well above those found *in situ* (Alves *et al.*, 2019). Given that both the direct and indirect roles of AOA in the cycling of N_2O in polar soils remain largely undetermined, a better understanding of polar microbial communities is paramount to model current and future N_2O fluxes from this biome.

Acknowledgments

This study was funded by the Academy of Finland (project 335354) and the University of Helsinki. We would like to acknowledge the CSC – IT Centre for Science, Finland, for providing computing resources; Miska Luoto and the BioGeoClimate Modelling Lab at the University of Helsinki for providing the Rásttigáisá samples; Eeva Eronen-Rasimus, Laura Cappelatti, and Benoit Durieu for helpful suggestions and discussions; and Jouko Rikkinen and Heino Vänskä for nomenclatural advice.

463 ## Data availability

464 Genomic assemblies can be found in GenBank/ENA under the accession numbers listed in
465 **Table 1**. MAGs generated in this study have been submitted to ENA (BioProject PRJEB49283).
466 All the code used can be found in https://github.com/ArcticMicrobialEcology/candidatus-
467 nitrosopolaris.

468 ## Author contributions

469 ISP, AR, and JH designed the study. ISP performed the analyses and wrote the manuscript. AR
470 and JH revised the manuscript.

471 ## Competing interests

472 The authors declare no conflict of interests.

473 ## References

474 Alves, R.J.E., Kerou, M., Zappe, A., Bittner, R., Abby, S.S., Schmidt, H.A., et al. (2019) Ammonia
475 Oxidation by the Arctic Terrestrial Thaumarchaeote Candidatus Nitrosocosmicus arcticus Is
476 Stimulated by Increasing Temperatures. *Front Microbiol* **10**: 1571.

477 Alves, R.J.E., Minh, B.Q., Urich, T., von Haeseler, A., and Schleper, C. (2018) Unifying the
478 global phylogeny and environmental distribution of ammonia-oxidising archaea based on amoA
479 genes. *Nat Commun* **9**: 1517.

480 Alves, R.J.E., Wanek, W., Zappe, A., Richter, A., Svenning, M.M., Schleper, C., and Urich, T.
481 (2013) Nitrification rates in Arctic soils are associated with functionally distinct populations of
482 ammonia-oxidizing archaea. *ISME J* **7**: 1620–1631.

483 Aramaki, T., Blanc-Mathieu, R., Endo, H., Ohkubo, K., Kanehisa, M., Goto, S., and Ogata, H.
484 (2020) KofamKOALA: KEGG Ortholog assignment based on profile HMM and adaptive score
485 threshold. *Bioinformatics* **36**: 2251–2252.

486 Bissett, A., Fitzgerald, A., Meintjes, T., Mele, P.M., Reith, F., Dennis, P.G., et al. (2016)
487 Introducing BASE: the Biomes of Australian Soil Environments soil microbial diversity
488 database. *GigaScience* **5**: 21.

489 Bowers, R.M., Kyrpides, N.C., Stepanauskas, R., Harmon-Smith, M., Doud, D., Reddy, T.B.K.,
490 et al. (2017) Minimum information about a single amplified genome (MISAG) and a
491 metagenome-assembled genome (MIMAG) of bacteria and archaea. *Nat Biotechnol* **35**: 725–731.

492 Bowman, J.P. (2013) Sea-Ice Microbial Communities. In *The Prokaryotes*. Rosenberg, E.,
493 DeLong, E.F., Lory, S., Stackebrandt, E., and Thompson, F. (eds). Berlin, Heidelberg: Springer
494 Berlin Heidelberg, pp. 139–161.

495 Buchfink, B., Xie, C., and Huson, D.H. (2015) Fast and sensitive protein alignment using
496 DIAMOND. *Nat Methods* **12**: 59–60.

497 Butterbach-Bahl, K., Baggs, E.M., Dannenmann, M., Kiese, R., and Zechmeister-Boltenstern,
498 S. (2013) Nitrous oxide emissions from soils: how well do we understand the processes and their
499 controls? *Philos Trans R Soc B Biol Sci* **368**: 20130122.

500 Camacho, C., Coulouris, G., Avagyan, V., Ma, N., Papadopoulos, J., Bealer, K., and Madden,
501 T.L. (2009) BLAST+: architecture and applications. *BMC Bioinformatics* **10**: 421.

502 Cavicchioli, R. (2006) Cold-adapted archaea. *Nat Rev Microbiol* **4**: 331–343.

503 Chauhan, A., Layton, A.C., Vishnivetskaya, T.A., Williams, D., Pfiffner, S.M., Rekepalli, B., et
504 al. (2014) Metagenomes from Thawing Low-Soil-Organic-Carbon Mineral Cryosols and
505 Permafrost of the Canadian High Arctic. *Genome Announc* **2**:.

506 Chaumeil, P.-A., Mussig, A.J., Hugenholtz, P., and Parks, D.H. (2019) GTDB-Tk: a toolkit to
507 classify genomes with the Genome Taxonomy Database. *Bioinformatics* btz848.

508 Ciufo, S., Kannan, S., Sharma, S., Badretdin, A., Clark, K., Turner, S., et al. (2018) Using
509 average nucleotide identity to improve taxonomic assignments in prokaryotic genomes at the
510 NCBI. *Int J Syst Evol Microbiol* **68**: 2386–2392.

511 Daebeler, A., Abell, G.C.J., Bodelier, P.L.E., Bodrossy, L., Frampton, D.M.F., Hefting, M.M.,
512 and Laanbroek, H.J. (2012) Archaeal dominated ammonia-oxidizing communities in Icelandic
513 grassland soils are moderately affected by long-term N fertilization and geothermal heating.
514 *Front Microbiol* **3**:.

515 Daims, H., Lebedeva, E.V., Pjevac, P., Han, P., Herbold, C., Albertsen, M., et al. (2015) Complete
516 nitrification by Nitrospira bacteria. *Nature* **528**: 504–509.

517 Eddy, S.R. (2011) Accelerated Profile HMM Searches. *PLoS Comput Biol* **7**: e1002195.

518 Edgar, R.C. (2004) MUSCLE: multiple sequence alignment with high accuracy and high
519 throughput. *Nucleic Acids Res* **32**: 1792–1797.

520 Edgar, R.C. (2010) Search and clustering orders of magnitude faster than BLAST.
521 *Bioinformatics* **26**: 2460–2461.

522 Eren, A.M., Esen, Ö.C., Quince, C., Vineis, J.H., Morrison, H.G., Sogin, M.L., and Delmont, T.O.
523 (2015) Anvi'o: an advanced analysis and visualization platform for 'omics data. *PeerJ* **3**: e1319.

524 Gadkari, P.S., McGuinness, L.R., Männistö, M.K., Kerkhof, L.J., and Häggblom, M.M. (2020)
525 Arctic tundra soil bacterial communities active at subzero temperatures detected by stable
526 isotope probing. *FEMS Microbiol Ecol* **96**: fiz192.

527 Galperin, M.Y., Wolf, Y.I., Makarova, K.S., Vera Alvarez, R., Landsman, D., and Koonin, E.V.
528 (2021) COG database update: focus on microbial diversity, model organisms, and widespread
529 pathogens. *Nucleic Acids Res* **49**: D274–D281.

530 Hayashi, K., Tanabe, Y., Fujitake, N., Kida, M., Wang, Y., Hayatsu, M., and Kudoh, S. (2020)
531 Ammonia Oxidation Potentials and Ammonia Oxidizers of Lichen–Moss Vegetated Soils at Two
532 Ice-free Areas in East Antarctica. *Microbes Environ* **35**: n/a.

533 Hwang, Y., Schulze-Makuch, D., Arens, F.L., Saenz, J.S., Adam, P.S., Sager, C., et al. (2021)
534 Leave no stone unturned: individually adapted xerotolerant Thaumarchaeota sheltered below
535 the boulders of the Atacama Desert hyperarid core. *Microbiome* **9**: 234.

536 Hyatt, D., Chen, G.-L., LoCascio, P.F., Land, M.L., Larimer, F.W., and Hauser, L.J. (2010)
537 Prodigal: prokaryotic gene recognition and translation initiation site identification. *BMC*
538 *Bioinformatics* **11**: 119.

539 Ji, M., Greening, C., Vanwonterghem, I., Carere, C.R., Bay, S.K., Steen, J.A., et al. (2017)
540 Atmospheric trace gases support primary production in Antarctic desert surface soil. *Nature*
541 **552**: 400–403.

542 Jung, M.-Y., Islam, Md.A., Gwak, J.-H., Kim, J.-G., and Rhee, S.-K. (2018) Nitrosarchaeum
543 koreense gen. nov., sp. nov., an aerobic and mesophilic, ammonia-oxidizing archaeon member
544 of the phylum Thaumarchaeota isolated from agricultural soil. *Int J Syst Evol Microbiol* **68**:
545 3084–3095.

546 Jung, M.-Y., Sedlacek, C.J., Kits, K.D., Mueller, A.J., Rhee, S.-K., Hink, L., et al. (2022)
547 Ammonia-oxidizing archaea possess a wide range of cellular ammonia affinities. *ISME J* **16**:
548 272–283.

549 Katoh, K. and Standley, D.M. (2013) MAFFT Multiple Sequence Alignment Software Version
550 7: Improvements in Performance and Usability. *Mol Biol Evol* **30**: 772–780.

551 Kerou, M., Offre, P., Valledor, L., Abby, S.S., Melcher, M., Nagler, M., et al. (2016) Proteomics
552 and comparative genomics of *Nitrososphaera viennensis* reveal the core genome and adaptations
553 of archaeal ammonia oxidizers. *Proc Natl Acad Sci* **113**: E7937–E7946.

554 Kim, M., Oh, H.-S., Park, S.-C., and Chun, J. (2014) Towards a taxonomic coherence between
555 average nucleotide identity and 16S rRNA gene sequence similarity for species demarcation of
556 prokaryotes. *Int J Syst Evol Microbiol* **64**: 346–351.

557 Kits, K.D., Sedlacek, C.J., Lebedeva, E.V., Han, P., Bulaev, A., Pjevac, P., et al. (2017) Kinetic
558 analysis of a complete nitrifier reveals an oligotrophic lifestyle. *Nature* **549**: 269–272.

559 Komárek, J., Ka□tovský, J., Ventura, S., and Turicchia, S. □marda (2009) The cyanobacterial
560 genus Phormidesmis. *Algol Stud* **129**: 41–59.

561 Könneke, M., Schubert, D.M., Brown, P.C., Hugler, M., Standfest, S., Schwander, T., et al.
562 (2014) Ammonia-oxidizing archaea use the most energy-efficient aerobic pathway for CO2
563 fixation. *Proc Natl Acad Sci* **111**: 8239–8244.

564 Konstantinidis, K.T., Rosselló-Móra, R., and Amann, R. (2017) Uncultivated microbes in need
565 of their own taxonomy. *ISME J* **11**: 2399–2406.

566 Lagkouvardos, I., Joseph, D., Kapfhammer, M., Giritli, S., Horn, M., Haller, D., and Clavel, T.
567 (2016) IMNGS: A comprehensive open resource of processed 16S rRNA microbial profiles for
568 ecology and diversity studies. *Sci Rep* **6**: 33721.

569 Langmead, B. and Salzberg, S.L. (2012) Fast gapped-read alignment with Bowtie 2. *Nat*
570 *Methods* **9**: 357–359.

571 Lehtovirta-Morley, L.E. (2018) Ammonia oxidation: Ecology, physiology, biochemistry and why
572 they must all come together. *FEMS Microbiol Lett* **365**:.

573 Lehtovirta-Morley, L.E., Ross, J., Hink, L., Weber, E.B., Gubry-Rangin, C., Thion, C., et al.
574 (2016) Isolation of ' *Candidatus* Nitrosocosmicus franklandus', a novel ureolytic soil archaeal
575 ammonia oxidiser with tolerance to high ammonia concentration. *FEMS Microbiol Ecol* **92**:
576 fiw057.

577 Lehtovirta-Morley, L.E., Stoecker, K., Vilcinskas, A., Prosser, J.I., and Nicol, G.W. (2011)
578 Cultivation of an obligate acidophilic ammonia oxidizer from a nitrifying acid soil. *Proc Natl*
579 *Acad Sci* **108**: 15892–15897.

580 Leininger, S., Urich, T., Schloter, M., Schwark, L., Qi, J., Nicol, G.W., et al. (2006) Archaea
581 predominate among ammonia-oxidizing prokaryotes in soils. *Nature* **442**: 806–809.

582 Li, D., Liu, C.-M., Luo, R., Sadakane, K., and Lam, T.-W. (2015) MEGAHIT: an ultra-fast single-
583 node solution for large and complex metagenomics assembly via succinct de Bruijn graph.
584 *Bioinformatics* **31**: 1674–1676.

585 Li, H. (2016) Minimap and miniasm: fast mapping and de novo assembly for noisy long
586 sequences. *Bioinformatics* **32**: 2103–2110.

587 Li, H., Handsaker, B., Wysoker, A., Fennell, T., Ruan, J., Homer, N., et al. (2009) The Sequence
588 Alignment/Map format and SAMtools. *Bioinformatics* **25**: 2078–2079.

589 Magalhães, C.M., Machado, A., Frank-Fahle, B., Lee, C.K., and Cary, S.C. (2014) The ecological
590 dichotomy of ammonia-oxidizing archaea and bacteria in the hyper-arid soils of the Antarctic
591 Dry Valleys. *Front Microbiol* **5**:.

592 Makarova, K., Wolf, Y., and Koonin, E. (2015) Archaeal Clusters of Orthologous Genes
593 (arCOGs): An Update and Application for Analysis of Shared Features between Thermococcales,
594 Methanococcales, and Methanobacteriales. *Life* **5**: 818–840.

595 Martens-Habbena, W., Berube, P.M., Urakawa, H., de la Torre, J.R., and Stahl, D.A. (2009)
596 Ammonia oxidation kinetics determine niche separation of nitrifying Archaea and Bacteria.
597 *Nature* **461**: 976–979.

598 Martin, M. (2011) Cutadapt removes adapter sequences from high-throughput sequencing
599 reads. *EMBnet.journal* **17**: 10.

600 Mistry, J., Chuguransky, S., Williams, L., Qureshi, M., Salazar, G.A., Sonnhammer, E.L.L., et
601 al. (2021) Pfam: The protein families database in 2021. *Nucleic Acids Res* **49**: D412–D419.

602 Mussmann, M., Brito, I., Pitcher, A., Sinninghe Damste, J.S., Hatzenpichler, R., Richter, A., et
603 al. (2011) Thaumarchaeotes abundant in refinery nitrifying sludges express amoA but are not
604 obligate autotrophic ammonia oxidizers. *Proc Natl Acad Sci* **108**: 16771–16776.

605 Nguyen, L.-T., Schmidt, H.A., von Haeseler, A., and Minh, B.Q. (2015) IQ-TREE: A Fast and
606 Effective Stochastic Algorithm for Estimating Maximum-Likelihood Phylogenies. *Mol Biol Evol*
607 **32**: 268–274.

608 O'Leary, N.A., Wright, M.W., Brister, J.R., Ciufo, S., Haddad, D., McVeigh, R., et al. (2016)
609 Reference sequence (RefSeq) database at NCBI: current status, taxonomic expansion, and
610 functional annotation. *Nucleic Acids Res* **44**: D733–D745.

611 Ortiz, M., Bosch, J., Coclet, C., Johnson, J., Lebre, P., Salawu-Rotimi, A., et al. (2020) Microbial
612 Nitrogen Cycling in Antarctic Soils. *Microorganisms* **8**: 1442.

613 Parks, D.H., Chuvochina, M., Chaumeil, P.-A., Rinke, C., Mussig, A.J., and Hugenholtz, P.
614 (2020) A complete domain-to-species taxonomy for Bacteria and Archaea. *Nat Biotechnol*.

615 Parks, D.H., Chuvochina, M., Waite, D.W., Rinke, C., Skarshewski, A., Chaumeil, P.-A., and
616 Hugenholtz, P. (2018) A standardized bacterial taxonomy based on genome phylogeny
617 substantially revises the tree of life. *Nat Biotechnol* **36**: 996–1004.

618 Parks, D.H., Rinke, C., Chuvochina, M., Chaumeil, P.-A., Woodcroft, B.J., Evans, P.N., et al.
619 (2017) Recovery of nearly 8,000 metagenome-assembled genomes substantially expands the tree
620 of life. *Nat Microbiol* **2**: 1533–1542.

621 Pessi, I.S., Osorio-Forero, C., Gálvez, E.J.C., Simões, F.L., Simões, J.C., Junca, H., and Macedo,
622 A.J. (2015) Distinct composition signatures of archaeal and bacterial phylotypes in the Wanda
623 Glacier forefield, Antarctic Peninsula. *FEMS Microbiol Ecol* **91**: 1–10.

624 Pessi, I.S., Viitamäki, S., Virkkala, A.-M., Eronen-Rasimus, E., Delmont, T.O., Marushchak,
625 M.E., et al. (2022) Truncated denitrifiers dominate the denitrification pathway in tundra soil
626 metagenomes. *bioRxiv*.

627 Pester, M., Schleper, C., and Wagner, M. (2011) The Thaumarchaeota: an emerging view of their
628 phylogeny and ecophysiology. *Curr Opin Microbiol* **14**: 300–306.

629 Pritchard, L., Glover, R.H., Humphris, S., Elphinstone, J.G., and Toth, I.K. (2016) Genomics
630 and taxonomy in diagnostics for food security: soft-rotting enterobacterial plant pathogens. *Anal*
631 *Methods* **8**: 12–24.

632 Qin, W., Heal, K.R., Ramdasi, R., Kobelt, J.N., Martens-Habbena, W., Bertagnolli, A.D., et al.
633 (2017) Nitrosopumilus maritimus gen. nov., sp. nov., Nitrosopumilus cobalaminigenes sp. nov.,
634 Nitrosopumilus oxyclinae sp. nov., and Nitrosopumilus ureiphilus sp. nov., four marine
635 ammonia-oxidizing archaea of the phylum Thaumarchaeota. *Int J Syst Evol Microbiol* **67**: 5067–
636 5079.

637 Raymond-Bouchard, I., Goordial, J., Zolotarov, Y., Ronholm, J., Stromvik, M., Bakermans, C.,
638 and Whyte, L.G. (2018) Conserved genomic and amino acid traits of cold adaptation in subzero-
639 growing Arctic permafrost bacteria. *FEMS Microbiol Ecol* **94**:.

640 Richter, I., Herbold, C.W., Lee, C.K., McDonald, I.R., Barrett, J.E., and Cary, S.C. (2014)
641 Influence of soil properties on archaeal diversity and distribution in the McMurdo Dry Valleys,
642 Antarctica. *FEMS Microbiol Ecol* **89**: 347–359.

643 Rinke, C., Chuvochina, M., Mussig, A.J., Chaumeil, P.-A., Davín, A.A., Waite, D.W., et al. (2021)
644 A standardized archaeal taxonomy for the Genome Taxonomy Database. *Nat Microbiol* **6**: 946–
645 959.

646 Rosselló-Móra, R. and Amann, R. (2015) Past and future species definitions for Bacteria and
647 Archaea. *Syst Appl Microbiol* **38**: 209–216.

648 Schleper, C. and Nicol, G.W. (2010) Ammonia-Oxidising Archaea – Physiology, Ecology and
649 Evolution. In *Advances in Microbial Physiology*. Elsevier, pp. 1–41.

650 Schloss, P.D. (2021) Amplicon Sequence Variants Artificially Split Bacterial Genomes into
651 Separate Clusters. *mSphere* **6**: e00191-21.

652 Shaiber, A., Willis, A.D., Delmont, T.O., Roux, S., Chen, L.-X., Schmid, A.C., et al. (2020)
653 Functional and genetic markers of niche partitioning among enigmatic members of the human
654 oral microbiome. *Genome Biol* **21**: 292.

655 Siljanen, H.M.P., Alves, R.J.E., Ronkainen, J.G., Lamprecht, R.E., Bhattarai, H.R., Bagnoud,
656 A., et al. (2019) Archaeal nitrification is a key driver of high nitrous oxide emissions from arctic
657 peatlands. *Soil Biol Biochem* **137**: 107539.

658 Spang, A., Poehlein, A., Offre, P., Zumbrägel, S., Haider, S., Rychlik, N., et al. (2012) The
659 genome of the ammonia-oxidizing *Candidatus* Nitrososphaera gargensis: insights into
660 metabolic versatility and environmental adaptations: The genome of *Candidatus*
661 Nitrososphaera gargensis. *Environ Microbiol* **14**: 3122–3145.

662 Stackebrandt, E. and Ebers, J. (2006) Taxonomic parameters revisited: tarnished gold
663 standards. *Microbiol Today* **33**: 152–155.

664 Stackhouse, B.T., Vishnivetskaya, T.A., Layton, A., Chauhan, A., Pfiffner, S., Mykytczuk, N.C.,
665 et al. (2015) Effects of simulated spring thaw of permafrost from mineral cryosol on CO_2
666 emissions and atmospheric CH_4 uptake. *J Geophys Res Biogeosciences* **120**: 1764–1784.

667 Stieglmeier, M., Klingl, A., Alves, R.J.E., Rittmann, S.K.-M.R., Melcher, M., Leisch, N., and
668 Schleper, C. (2014) Nitrososphaera viennensis gen. nov., sp. nov., an aerobic and mesophilic,
669 ammonia-oxidizing archaeon from soil and a member of the archaeal phylum Thaumarchaeota.
670 *Int J Syst Evol Microbiol* **64**: 2738–2752.

671 Strunecky, O., Raabova, L., Bernardova, A., Ivanova, A.P., Semanova, A., Crossley, J., and
672 Kaftan, D. (2020) Diversity of cyanobacteria at the Alaska North Slope with description of two
673 new genera: Gibliniella and Shackletoniella. *FEMS Microbiol Ecol* **96**: fiz189.

674 Tahon, G., Geesink, P., and Ettema, T.J.G. (2021) Expanding Archaeal Diversity and
675 Phylogeny: Past, Present, and Future. *Annu Rev Microbiol* **75**: 359–381.

676 The UniProt Consortium (2019) UniProt: a worldwide hub of protein knowledge. *Nucleic Acids*
677 *Res* **47**: D506–D515.

678 de la Torre, J.R., Walker, C.B., Ingalls, A.E., Könneke, M., and Stahl, D.A. (2008) Cultivation
679 of a thermophilic ammonia oxidizing archaeon synthesizing crenarchaeol. *Environ Microbiol* **10**:
680 810–818.

681 Voigt, C., Marushchak, M.E., Abbott, B.W., Biasi, C., Elberling, B., Siciliano, S.D., et al. (2020)
682 Nitrous oxide emissions from permafrost-affected soils. *Nat Rev Earth Environ* **1**: 420–434.

683 Wang, Q., Zhu, R., Zheng, Y., Bao, T., and Hou, L. (2019) Effects of sea animal colonization on
684 the coupling between dynamics and activity of soil ammonia-oxidizing bacteria and archaea in
685 maritime Antarctica. *Biogeosciences* **16**: 4113–4128.

686 Wu, L., Chen, X., Wei, W., Liu, Y., Wang, D., and Ni, B.-J. (2020) A Critical Review on Nitrous
687 Oxide Production by Ammonia-Oxidizing Archaea. *Environ Sci Technol* **54**: 9175–9190.

688 Xie, Z., Le Roux, X., Wang, C., Gu, Z., An, M., Nan, H., et al. (2014) Identifying response groups
689 of soil nitrifiers and denitrifiers to grazing and associated soil environmental drivers in Tibetan
690 alpine meadows. *Soil Biol Biochem* **77**: 89–99.

691 Yang, Y., Zhang, C., Lenton, T.M., Yan, X., Zhu, M., Zhou, M., et al. (2021) The Evolution
692 Pathway of Ammonia-Oxidizing Archaea Shaped by Major Geological Events. *Mol Biol Evol* **38**:
693 3637–3648.

694 Yarza, P., Yilmaz, P., Pruesse, E., Glöckner, F.O., Ludwig, W., Schleifer, K.-H., et al. (2014)
695 Uniting the classification of cultured and uncultured bacteria and archaea using 16S rRNA gene
696 sequences. *Nat Rev Microbiol* **12**: 635–645.

697 Zhang, S., Xia, X., Li, S., Zhang, L., Wang, G., Li, M., et al. (2019) Ammonia Oxidizers in High-
698 Elevation Rivers of the Qinghai-Tibet Plateau Display Distinctive Distribution Patterns. *Appl*
699 *Environ Microbiol* **85**:.

700 # SSupplementary Information

701 **Suppl. Table S1 (separate .xlsx file).** Additional information on metagenome-assembled
702 genomes (MAGs) belonging to the UBA10452 lineage (*Candidatus* Nitrosopolaris).

703 **Suppl. Table S2 (separate .xlsx file).** Information about selected genes used for the
704 reconstruction of the metabolic potential of the UBA10452 lineage (*Candidatus* Nitrosopolaris).

705 **Suppl. Table S3 (separate .xlsx file).** arCOG functions enriched in metagenome-assembled
706 genomes (MAGs) belonging to the UBA10452 lineage (*Candidatus* Nitrosopolaris).

707 **Suppl. Table S4 (separate .xlsx file).** Genes with known or predicted roles in cold adaptation
708 and growth found in metagenome-assembled genomes (MAGs) belonging to the UBA10452
709 lineage (*Candidatus* Nitrosopolaris).

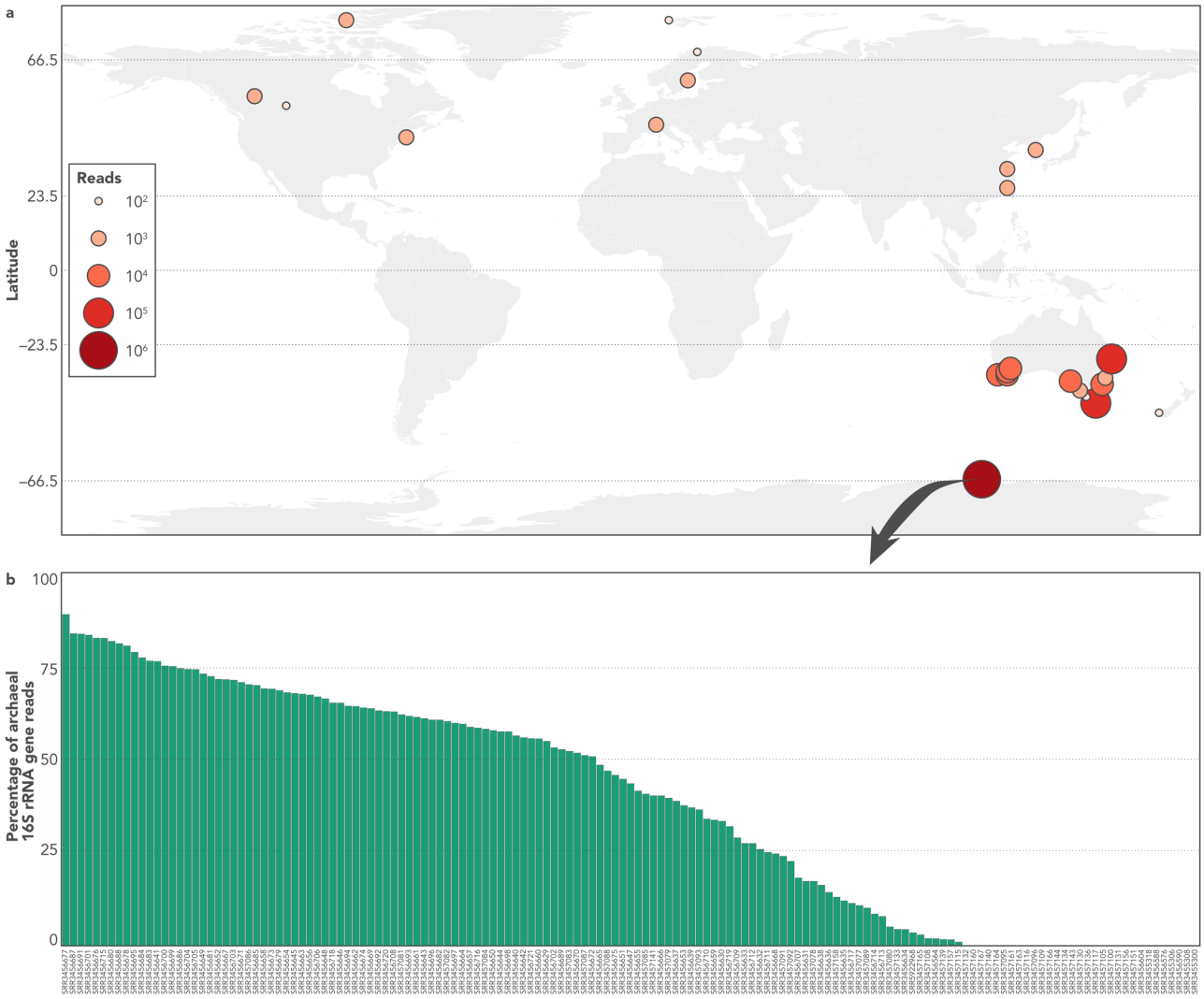

Suppl. Figure S1. Geographic distribution of the UBA10452 lineage (*Candidatus* Nitrosopolaris). a) Distribution of *Ca.* Nitrosopolaris based on the screening of 422,877 16S rRNA gene amplicon sequencing datasets in the Sequence Read Archive (SRA). Datasets with few matches (< 0.1% or < 100 reads) are not shown. **b)** Abundance of *Ca.* Nitrosopolaris across 149 16S rRNA gene amplicon sequencing datasets from soils in the vicinity of Davis Station, Princess Elizabeth Land, Antarctica (BioProject PRJNA317932). Relative abundances were computed as the proportion of reads matching the sequence of *Ca.* Nitrosopolaris in each sample. Abundances represent the percentage of *Ca.* Nitrosopolaris reads relative to archaeal 16S rRNA gene reads obtained with archaea-specific primers.

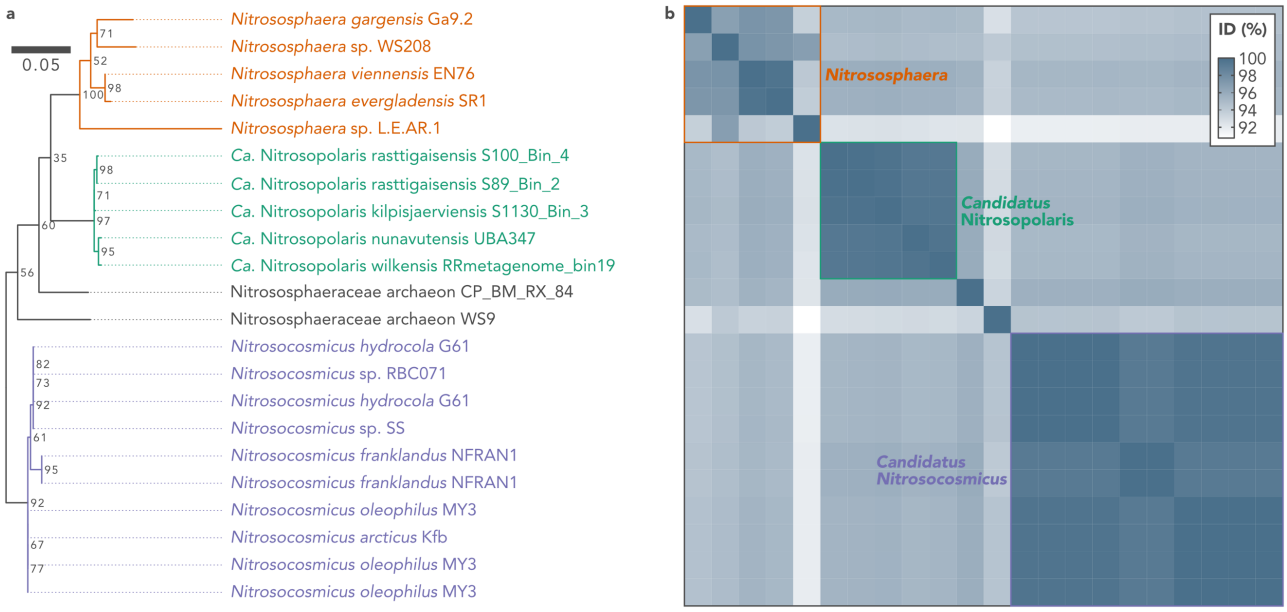

Suppl. Figure S2. The 16S rRNA gene of UBA10452 (*Candidatus* Nitrosopolaris). a) Phylogenetic analysis of the 16S rRNA gene sequence of five metagenome-assembled genomes (MAGs) assigned to the UBA10452 lineage and other Nitrososphaeraceae genomes available on GenBank. Maximum likelihood tree rooted with *Nitrosopumilus maritimus* SCM1 (not shown). Bootstrap values for node support are indicated. **b)** Pairwise similarity between 16S rRNA gene sequences. Note that some genomes contain multiple copies of the 16S rRNA gene.

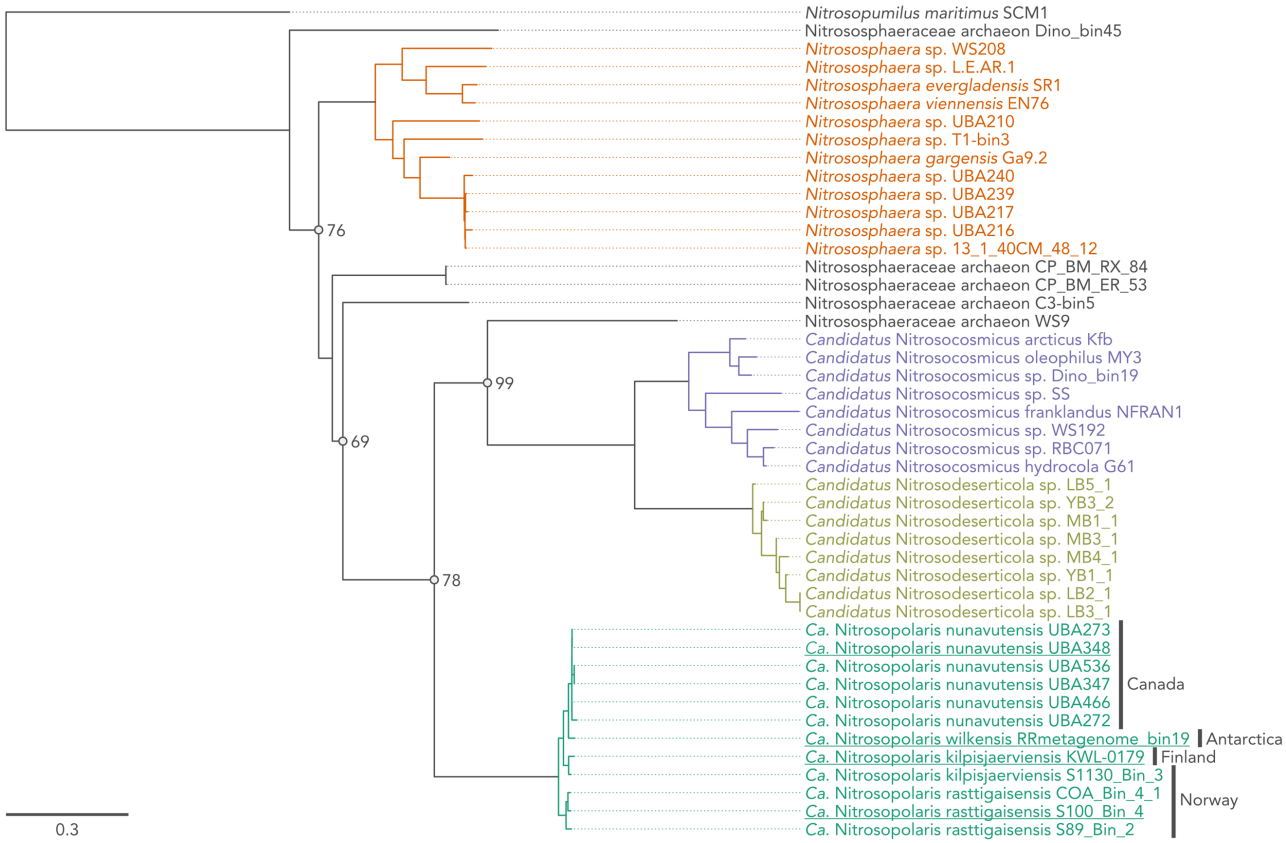

Suppl. Figure S3. Phylogenomic analysis of the UBA10452 lineage (*Candidatus* Nitrosopolaris). Maximum likelihood tree based on 59 single-copy genes from 12 metagenome-assembled genomes (MAGs) assigned to the UBA10452 lineage and 33 other Nitrososphaeraceae genomes available on GenBank. *Nitrosopumilus maritimus* SCM1 was used for rooting the tree. Nodes are supported by bootstrap values of 100% unless shown otherwise. Representatives for the four proposed species are indicated in underscore. This is an uncollapsed and bootstrapped version of the tree found in **Fig. 2a**.

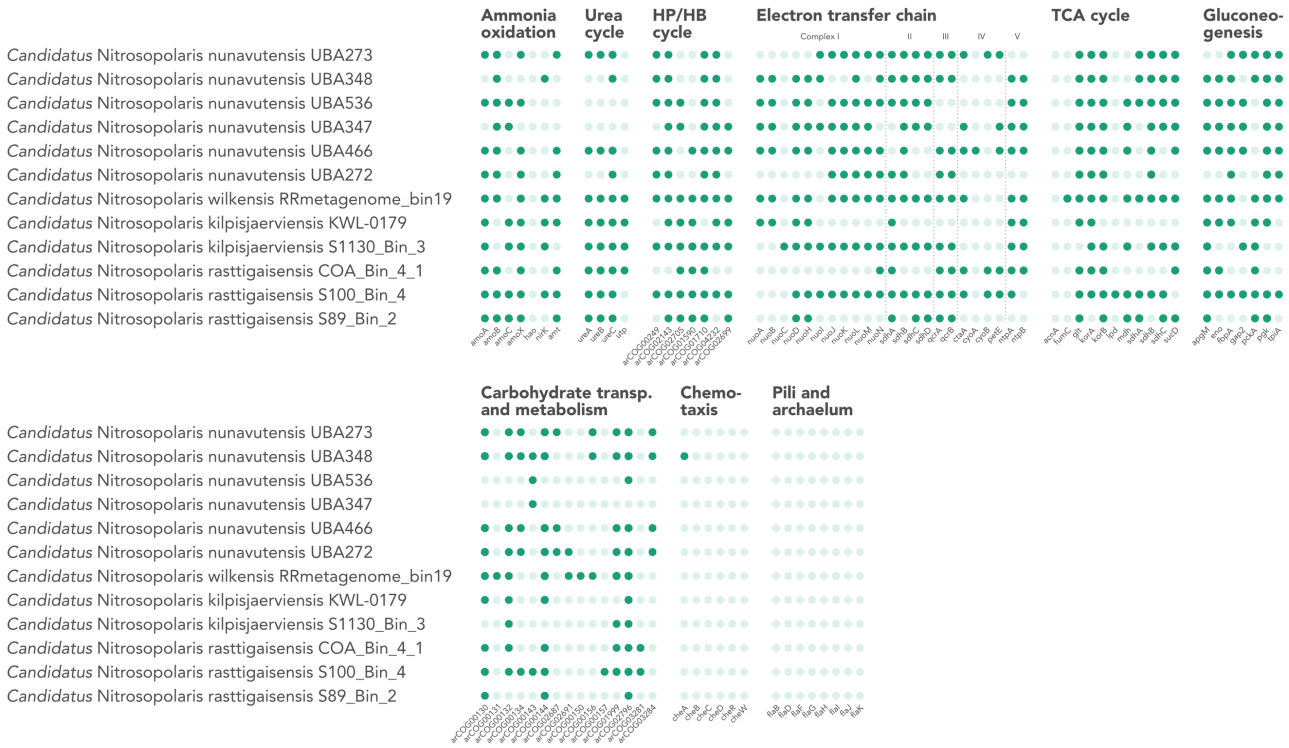

Suppl. Figure S4. Metabolic potential of the UBA10452 lineage (*Candidatus* Nitrosopolaris). Metabolic potential was estimated based on the presence of key genes involved in selected pathways. Detailed information about the genes can be found in **Suppl. Table S2**.

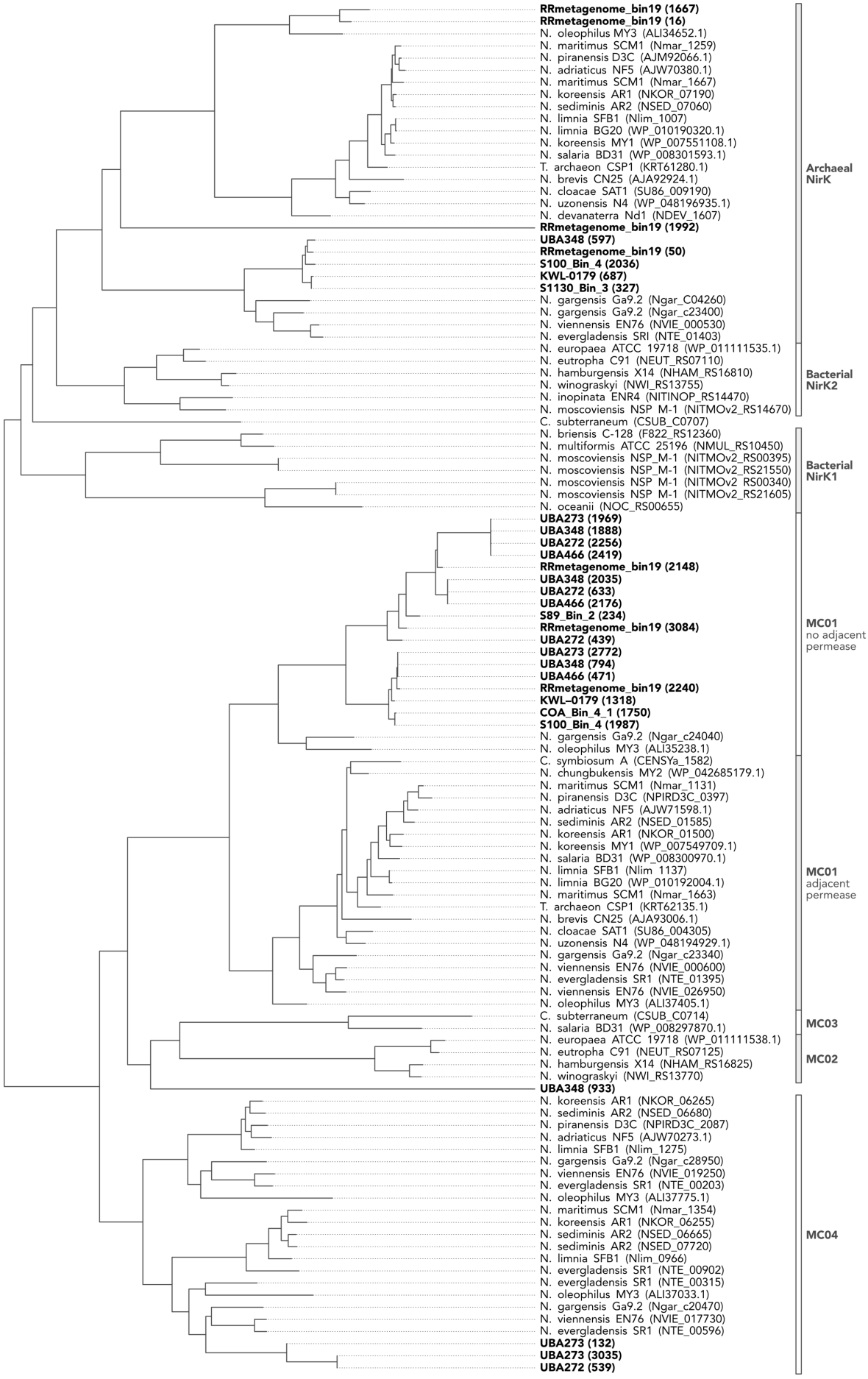
RRmetagenome_bin19 (1667)
RRmetagenome_bin19 (16)
N. oleophilus MY3 (ALI34652.1)
N. maritimus SCM1 (Nmar_1259)
N. piranensis D3C (AJM92066.1)
N. adriaticus NF5 (AJW70380.1)
N. maritimus SCM1 (Nmar_1667)
N. koreensis AR1 (NKOR_07190)
N. sediminis AR2 (NSED_07060)
N. limnia SFB1 (Nlim_1007)
N. limnia BG20 (WP_010190320.1)
N. koreensis MY1 (WP_007551108.1)
N. salaria BD31 (WP_008301593.1)
T. archaeon CSP1 (KRT61280.1)
N. brevis CN25 (AJA92924.1)
N. cloacae SAT1 (SU86_009190)
N. uzonensis N4 (WP_048196935.1)
N. devanaterra Nd1 (NDEV_1607)
RRmetagenome_bin19 (1992)
UBA348 (597)
RRmetagenome_bin19 (50)
S100_Bin_4 (2036)
KWL-0179 (687)
S1130_Bin_3 (327)
N. gargensis Ga9.2 (Ngar_C04260)
N. gargensis Ga9.2 (Ngar_c23400)
N. viennensis EN76 (NVIE_000530)
N. evergladensis SRI (NTE_01403)
N. europaea ATCC 19718 (WP_011111535.1)
N. eutropha C91 (NEUT_RS07110)
N. hamburgensis X14 (NHAM_RS16810)
N. winograskyi (NWI_RS13755)
N. inopinata ENR4 (NITINOP_RS14470)
N. moscoviensis NSP M-1 (NITMOv2_RS14670)
C. subterraneum (CSUB_C0707)
N. briensis C-128 (F822_RS12360)
N. multiformis ATCC 25196 (NMUL_RS10450)
N. moscoviensis NSP_M-1 (NITMOv2_RS00395)
N. moscoviensis NSP_M-1 (NITMOv2_RS21550)
N. moscoviensis NSP M-1 (NITMOv2 RS00340)
N. moscoviensis NSP M-1 (NITMOv2_RS21605)
N. oceanii (NOC_RS00655)
UBA273 (1969)
UBA348 (1888)
UBA272 (2256)
UBA466 (2419)
RRmetagenome_bin19 (2148)
UBA348 (2035)
UBA272 (633)
UBA466 (2176)
S89_Bin_2 (234)
RRmetagenome_bin19 (3084)
UBA272 (439)
UBA273 (2772)
UBA348 (794)
UBA466 (471)
RRmetagenome_bin19 (2240)
KWL–0179 (1318)
COA_Bin_4_1 (1750)
S100_Bin_4 (1987)
N. gargensis Ga9.2 (Ngar_c24040)
N. oleophilus MY3 (ALI35238.1)
C. symbiosum A (CENSYa_1582)
N. chungbukensis MY2 (WP_042685179.1)
N. maritimus SCM1 (Nmar_1131)
N. piranensis D3C (NPIRD3C_0397)
N. adriaticus NF5 (AJW71598.1)
N. sediminis AR2 (NSED_01585)
N. koreensis AR1 (NKOR_01500)
N. koreensis MY1 (WP_007549709.1)
N. salaria BD31 (WP_008300970.1)
N. limnia SFB1 (Nlim 1137)
N. limnia BG20 (WP_010192004.1)
N. maritimus SCM1 (Nmar_1663)
T. archaeon CSP1 (KRT62135.1)
N. brevis CN25 (AJA93006.1)
N. cloacae SAT1 (SU86_004305)
N. uzonensis N4 (WP_048194929.1)
N. gargensis Ga9.2 (Ngar_c23340)
N. viennensis EN76 (NVIE_000600)
N. evergladensis SR1 (NTE_01395)
N. viennensis EN76 (NVIE_026950)
N. oleophilus MY3 (ALI37405.1)
C. subterraneum (CSUB_C0714)
N. salaria BD31 (WP_008297870.1)
N. europaea ATCC 19718 (WP_011111538.1)
N. eutropha C91 (NEUT_RS07125)
N. hamburgensis X14 (NHAM_RS16825)
N. winograskyi (NWI_RS13770)
UBA348 (933)
N. koreensis AR1 (NKOR_06265)
N. sediminis AR2 (NSED_06680)
N. piranensis D3C (NPIRD3C_2087)
N. adriaticus NF5 (AJW70273.1)
N. limnia SFB1 (Nlim_1275)
N. gargensis Ga9.2 (Ngar_c28950)
N. viennensis EN76 (NVIE_019250)
N. evergladensis SR1 (NTE_00203)
N. oleophilus MY3 (ALI37775.1)
N. maritimus SCM1 (Nmar_1354)
N. koreensis AR1 (NKOR_06255)
N. sediminis AR2 (NSED_06665)
N. sediminis AR2 (NSED_07720)
N. limnia SFB1 (Nlim_0966)
N. evergladensis SR1 (NTE_00902)
N. evergladensis SR1 (NTE_00315)
N. oleophilus MY3 (ALI37033.1)
N. gargensis Ga9.2 (Ngar_c20470)
N. viennensis EN76 (NVIE_017730)
N. evergladensis SR1 (NTE_00596)
UBA273 (132)
UBA273 (3035)
UBA272 (539)
Archaeal NirK
Bacterial NirK2
Bacterial NirK1
MC01 no adjacent permease
MC01 adjacent permease
MC03
MC02
MC04

737

(Previous page) Suppl. Figure S5. Phylogenetic analysis of putative NirK sequences from metagenome-assembled genomes (MAGs) belonging to the UBA10452 lineage (*Candidatus* Nitrosopolaris). Sequences from the UBA10452 are shown in bold and respective gene calls are given inside parenthesis. Other sequences were retrieved from Kerou *et al*. (2016).